RSC Advances

ROYAL SOCIETY OF CHEMISTRY

www.rsc.org/advances

Single-Layer Graphyne Membranes for Super-Excellent Brine Separation in Forward Osmosis

Xin Zhang and Jing-Gang Gai*

State Key Laboratory of Polymer Materials Engineering, Polymer Research Institute of Sichuan University, Chengdu, Sichuan 610065, China

Abstract

Forward osmosis (FO) technology has shown great promise in sea water desalinization and in power generation from the mixing of fresh water and seawater in estuaries. However, the desalination efficiency and the power density level of the present FO system are very low owing to the low water flux of the commercial FO membranes. In this study, we report the brine separation performance of single-layer graphyne-N (N=3, 4, 5, 6) membranes in forward osmosis system by molecular dynamic simulation. Our calculations show that graphyne-3 not only can achieve a high water flux up to about 39.15 L/(cm^2·h), which is 3 to 4 orders of magnitude higher than that of the conventional osmotic membranes, but also can achieve a perfect salt rejection rate. Results indicate that structural characteristics and charge properties of these membranes as well as the distribution pattern of both water molecules and salt ions in each system are the main factors that affect the brine separation performance of graphyne membranes. Besides, we find that the formation of hydrated salt ions is the basic reason of brine separation in salt solutions. Graphyne membranes have good prospects in brine separation, regeneration-free applications

* Corresponding authors. Tel.: +86 28 85467166; fax: +86 28 85402465. E-mail addresses: gaijinggang@scu.edu.cn (J-G. Gai)

and high salinity applications in FO.

Introduction

Water crisis is spreading to more and more countries and regions, owing to population growth, changes in rainfall patterns, environmental pollution, [1-4] etc. A report of the United Nations predicted that two-thirds of the population would face water crisis by 2025, [5, 6] which stimulates many countries to target at brine separation to release the increasingly severe water crisis. The methods of brine separation gradually develop from traditional heating which demands for high energy consumption and high investment in equipment, such as the multi-effect evaporation and multi-stage flash, to ways using membranes which are easy to operate and require low energy consumption. [7]

Currently, reverse osmosis (RO) occupies an important position in brine separation due to its relatively low energy consumption, flexible installation, lesser to corrosion and scaling, as well as low one-time investment. Nevertheless, there are still some problems in RO process, such as the short life of membranes and low water recovery rate, [8, 9] which lead forward osmosis (FO) to become a new hot spot.

In FO system, the two sides of the semipermeable membrane are respectively filled with feed solution and draw solution. Water molecules on the feed solution side spontaneously diffuse to the draw solution side relying on osmotic pressure difference. After that, the separation of draw solution can obtain pure water. [9-11] FO needs no external pressure, so the membrane fouling is much smaller than that of RO. The water recovery rate of FO is over 75% while that is 35%-50% for RO. [11] FO has great

value not only in the field of brine separation but also in other fields like conservation and reuse of osmosis energy. [10, 12]

The researches on FO membranes, one of the most important part of FO systems [13-16], are in full swing today. An ideal FO membrane must ensure a high water flux and a high salt rejection rate. [13] The brine separation performance of FO membranes can be improved by grafting some kinds of hydrophilic groups onto the active layer or support layer to ameliorate the hydrophilicity of the membranes. [14-17] Some researchers add pore-forming agent [17-20] into film-forming solution to increase the porosity of the support layer and adjust the bending factor of the holes, others try to reduce the thickness of the support layer by directly embedding polyester mesh into the polymer membranes. [20, 21] However, those membranes still cannot satisfy the actual requirements for brine separation.

The concentration polarization phenomenon (CP) [22, 23] is an important factor hindering the achievement of high separation performance of FO membranes. Especially, the inner concentration polarization (ICP) occurring in the support layer leads water flux to decrease by up to 80%. [23] Considering that water flux is inversely proportional to the thickness of the membrane, reducing the thickness of membranes can greatly increase water flux. However, if the support layer is removed or the membrane thickness is reduced significantly, the mechanical strength of the membranes cannot meet requirements. Therefore, an entry point in solving the problem is to explore new porous membranes with both high enough mechanical strength and ultrathin thickness to maximally minimize the mass transfer resistance of

water molecules and the influence of CP on the membrane performance.

Relevant researches show that carbon nanotubes (CNTs) and boron nitride nanotubes which possess hollow structures can achieve ultra-fast water transport performance and good salt rejection, [24-30] but it's difficult to form nanotube membranes by vertically arranging the nanotubes. In some research works, CNTs are embedded in polymer membranes, but the CP impact has not been reduced or eliminated on account of the existence of the polymer membranes. [26-29] In order to minimize the CP phenomenon, an ultrathin porous membrane with high mechanical strength is undoubtedly an excellent choice.

In some reports, the mechanical properties and permeability of single-layer graphene or modified graphene porous membranes, such as graphene nitride, graphene fluoride, graphene oxide, were studied using molecular simulations. [30-37] Molecular simulation results show that these porous membranes not only have high mechanical properties but also can achieve a high water flux and a high salt rejection rate in FO. With the rapid development of graphene material, there have been many inspiring breakthroughs in the fabrication of single-layer graphene membranes [38-42] since they were discovered in 2004 in the laboratory. Even more exciting, a high-quality graphene film which consists of predominantly single-layer graphene [42] has been successfully fabricated by roll-to-roll chemical vapor deposition (CVD) synthesis on a suspended copper foil under the condition of 1000 °C and low pressure. The length can reach up to 100 m and the width can reach about 210 mm. Several researchers have shown the feasibility of using single-layer porous graphene in brine

separation or desalination [43-45] by experiment. For example, in one research [43], the water transport properties of various plasma-etched single-layer graphene membranes were measured using four configurations and the resulting membranes exhibit a salt rejection rate of nearly 100% and fast water transport. Nevertheless, single-layer graphene membrane is non-porous and need drilling, and it is difficult to precisely control the size and distribution of the pores in practice. [35-37]

Graphyne, which is a carbon allotrope, has the same hexagonal symmetry as graphene. Graphyne-N (N = 1, 2, 3, …) are obtained by connecting N acetylenic bonds among the adjacent six-membered rings of graphene [46-56] and the effective Van der Waals pore diameter of graphyne-N increases with the increase of N. [48, 49] Researches by molecular simulation show that single-layer graphyne-N (N = 3, 4, 5, 6) membrane has high mechanical strength, its Young's modulus reaches up to 365-700 GPa, the uniaxially stretched final strength reaches up to 25-100 GPa and the ultimate uniaxial tensile strain is over 6%, which are sufficient for them to withstand the stress and deformation in clamping process or the external pressure when used in RO. Graphyne-N (N = 3, 4, 5, 6) membranes also hold excellent chemical stability and thermal stability. [48-56]

There have been some inspiring reports showing the successful synthesis of flake graphyne structures [57-59]. Most strikingly, Li et al. [60] report that graphdiyne films with the area of 3.61 cm^2 have been successfully fabricated on the surface of copper via a cross-coupling reaction using hexaethynylbenzene. The synthesizing and fabrication of graphyne have attracted more and more attentions due to its exceptional structure,

excellent mechanical and electrical properties. Furthermore, compared with graphene membranes, the pores of graphyne membranes are naturally formed, the complicated process of preparing pores can be avoided and the fabrication of single-layer graphyne membranes is more energy-saving. The natural regularity and the uniform distribution of those holes create an excellent condition for graphyne-N (N = 3, 4, 5, 6) membranes to achieve high separation performance. Just as the synthesis and fabrication of large-area graphene membranes develop rapidly thanks to the hard work of experimentalists, the successful fabrication of larger high-quality single-layer graphyne membranes with lower energy consuming is also promising. Considering that using single-layer porous graphene in brine separation or desalination is feasible, it's also promising to use single-layer graphyne membranes in these fields. Although scaling up these membranes for use in practical application remains a significant challenge, it is promising to be realized in the near future with the sustained efforts of researchers.

At present, only a few researchers have studied the performance of graphyne membranes in water treatment by molecular simulation. [46-50] Kou et al. [46] reported that the net water flux through the monolayer graphyne-3 membrane was much higher than that through the CNT membrane with similar nanopore diameter and the remarkable hydraulic permeability was attributed to the hydrogen bond formation. Their group also showed in another paper [49] that the water permeability and salt rejection of graphyne were closely related to the type of graphyne membrane, the salt concentration of solution and hydrostatic pressure. Zhu et al. [47] showed that water

permeability through graphyne exhibited nonlinear dependence on the pore size and they attributed this counter-intuitive behavior to the quantized nature of water flow at the nanoscale. Lin et al. [48] showed that hydrophobic graphyne membranes exhibited higher rejection rates for hydrophilic contaminants compared to the hydrophobic ones and that the size exclusion effect resulted in the different rejection rates. Xue et al. [50] reported that pristine graphyne could achieve complete rejection of nearly all ions in seawater and this resulted from the higher energy barriers for ions than for water. Nevertheless, these studies all are aimed at the separation performance of graphyne membranes in RO process and the effect of the charge properties of graphyne membranes on water permeability and on salt rejection have not been considered.

In this work, brine separation performance of single-layer graphyne-N (N = 3, 4, 5, and 6) membranes in FO have been studied by molecular dynamics (MD) simulation. The results show that single-layer graphyne membranes can not only achieve high water flux but also high salt rejection rates. We study the reasons for their high brine separation performance by analyzing the law of the diffusion and distribution of water molecules and salt ions in these systems as well as the effect of the charge properties of graphyne-N membranes on water permeability and salt rejection.

Simulation details

In this study, MD simulations were used to obtain the information about the brine separation performance of the single-layer graphyne-N (N = 3, 4, 5, and 6) membranes in FO systems. Pure water was chosen as feed solution and sodium

chloride solution with the mass percent concentration of 5% was adopted as draw solution, the structure of graphyne-N (N = 3, 4, 5, 6) membranes and the system for simulation are shown in Fig. 1.

The MD simulations were performed on unit cells containing graphyne-N (N = 3, 4, 5, 6) membranes. The modeling details are described as follows: Firstly, graphyne-N models were respectively built in single-layer, and we got the corresponding cubic unit cell box and set the length of c axis at 50 Å. The single-layer graphyne membranes always locate in the middle and are perpendicular to c axis. Secondly, energy minimization was performed to optimize the cell structure. Finally, pure water and salt solutions with the mass percent concentration of 5% were respectively filled into the two spaces on both sides of every membrane.

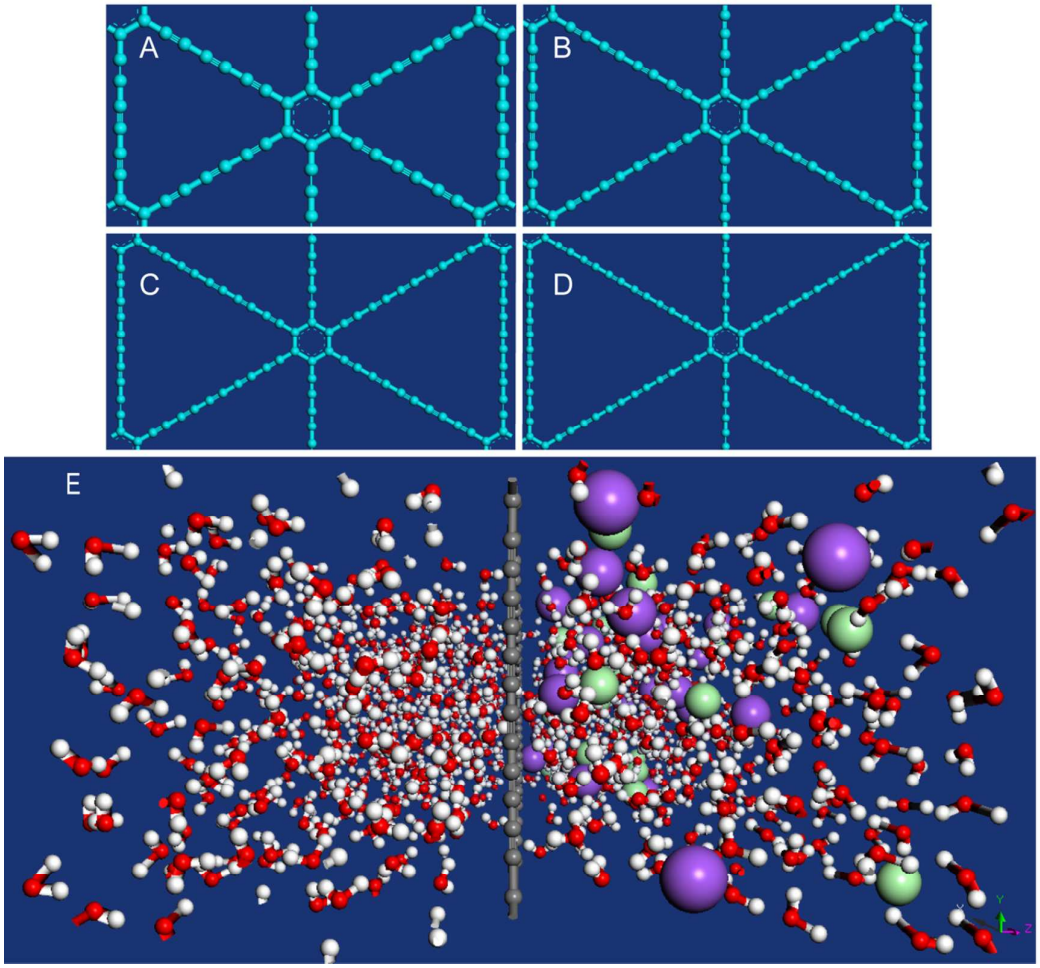

Fig. 1 Four graphyne membranes used in this simulation, (A) graphyne-3, (B) graphyne-4, (C) graphyne-5, (D) graphyne-6. (E) A snapshot of the simulation framework. The gray cycles are the carbon atoms of the graphyne membrane. Sodium chlorides are shown in sphere representation and in CPK style with Na^+ in purple and Cl^- in green. Water molecules are described by spheres with oxygen in red and hydrogen in white.

The COMPASS force field was used and the charge of each atom was determined by the Forcefield Assigned methods, Ewald and Atom Based methods were used to calculate the electrostatic and Van der Waals effects, respectively.

Afterwards, Smart Minimizer method was used to perform energy minimization for 5000 steps so as to get the lowest-energy conformation of every system.

MD simulations were running for 5 ns with the time step of 1 fs, and they were performed on the initial configurations which had been carried out energy minimization. To try to meet the actual FO operating conditions, the NPT ensemble was chose and thermostat was used to keep the temperature of the system constant at 298 K. The Nose mode was adopted to perform the fixed temperature calculation. This mode is more stable than the Andersen method for temperature control and it can be used to adjust the temperature for the system which is not balanced while the Andersen method is more adaptable to the systems under thermal equilibrium. The Berendsen method was adopted to keep the external pressure constant at 1 atm. The force field adopted for the molecular dynamics calculations is COMPASS, the charges were distributed by using the forcefield assigned methods, and both the electrostatic and the Van der Waals effects were calculated by the Ewald method.

Results and discussion

3.1 Water flux and salt rejection

Simulations were operated using the unit cell of single-layer graphyne-N (N = 3, 4, 5, 6) membranes. Both water flux and rejection rate were calculated using the final statistical results of 5 ns and each system was simulated for three times. Rejection rates were calculated using the formula

$$R = \left(1 - \frac{c_{jl}}{c_{jo}}\right) \times 100\% \quad (3.1)$$

Where R is rejection coefficient which is a measure of the ability of the membrane to

inversely reject salt ions from the draw solution in our systems, c_{jl} is the permeate concentration and c_{jo} is the initial concentration of draw solution. For a perfectly selective membrane, $c_{jl} = 0$ and $R = 100\%$, and for a completely unselective membrane, $c_{jl} = c_{jo}$ and $R = 0$. We have calculated the average values of the three simulation results for the water flux and rejection rate of each system, results are showed in Fig. 2, the fluctuation of the results displayed by the error bars are also showed in these water flux and rejection rate curves. We can get that in FO process, graphyne-3 has an average water flux up to about 39.15 L/(cm^2·h), which is 3 to 4 orders of magnitude higher than that of the industrial RO or FO membranes, [7-16, 18-21] and the salt rejection rate maintains 100% in the whole simulation process. Graphyne-4, graphyne-5 and graphyne-6 membranes have fluxes that are on the same order of magnitude as graphyne-3, but they cannot reach the ideal salt rejection as graphyne-3 membrane. They can be used in brine separation of lower salt rejection requirements or wastewater treatment with larger pollutant molecules.

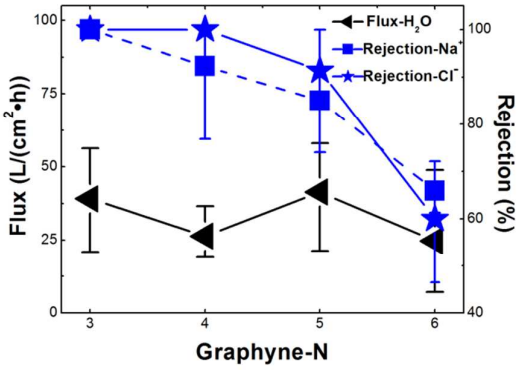

Fig. 2 Water flux (triangle), rejection of Na^+ (square) and Cl^- (pentagram) *vs* graphyne membrane type, namely graphyne-N (N=3, 4, 5, 6).

3.2 Water transport in the FO systems of single-layer graphyne membranes

According to Richard W. Baker, [61] the solution-diffusion model or the pore-flow model can be used to describe the mechanism of permeation. In the solution-diffusion model, permeants dissolve in the membrane and then diffuse through the membrane down a concentration gradient. Solution-diffusion model usually applies to polymeric membranes, because the free-volume elements of polymers, namely the inter-chain voids appear and disappear on around the same timescale as the motions of the permeants traversing the membrane, permeants can dissolve into these inter-chain voids and are separated by their different solubilities and diffusion rates. In pore-flow model, permeants transport through the tiny pores relying on the pressure-driven convective flow and they are separated by molecular filtration. Pore-flow model is usually applied to microporous membranes of which the pores do not fluctuate in position or volume on the timescale of permeant motion, these pores are relatively large and fixed and are connected to one another.

Graphyne-N (N = 3, 4, 5, 6) membranes are rigid and the pores of these membranes are relatively large and fixed, and the pore-flow model is more reasonable to be applied here to describe the water transport mechanism of graphyne-N membranes in FO. In these four systems, the temperature and the pressure as well as the initial osmotic pressure difference are the same. Three parameters can be used to characterize the structure complexity of graphyne-N membranes according to the theory of the pore flow model, namely membrane porosity, membrane tortuosity and the pore diameter. It is obvious that the porosity and pore diameter of graphyne-N membranes gradually increase with the increase of N and the tortuosity of graphyne-N

membranes are the same to each other. Fig. 2 shows that the water fluxes of graphyne-N (N=3, 4, 5, 6) membranes are in the same order of magnitude. There are no linear correlation between the water flux and the structure parameters including pore diameter and membrane porosity for graphyne-N membrane systems in FO.

To further study the effect of the charge property of each graphyne-N (N=3, 4, 5, 6) membrane on the water transport, we conducted the molecular dynamic simulations by changing the charges of all the carbon atoms on graphyne-N (N=3, 4, 5, 6) membranes to be zero and other settings are consistent with that of the previous four graphyne-N membrane systems. The simulation results are showed in Fig. 3. We can get from Fig. 3 that the water flux of graphyne-N membrane is higher than that of the corresponding uncharged graphyne-N membrane, especially for N = 3 and N = 6. It can be concluded that the charge properties of graphyne-N (N=3, 4, 5, 6) membranes are beneficial to the water transport in these FO systems.

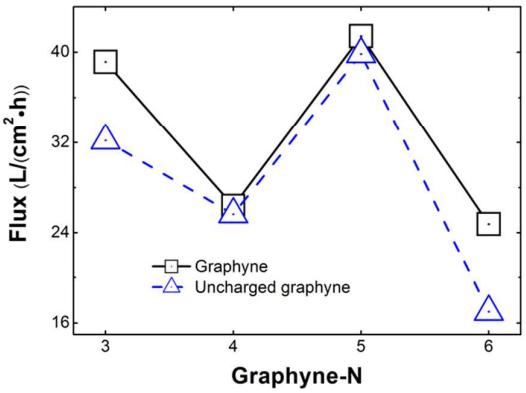

Fig. 3 Water flux of graphyne membrane and uncharged graphyne membrane *vs* membrane type, namely graphyne-N (N=3, 4, 5, 6).

Fig. 4 (a) and (b) respectively shows the mean square displacement (MSD) curves of water molecules with time varying in these four systems of graphyne-N

(N=3, 4, 5, 6) membranes and uncharged graphyne-N (N=3, 4, 5, 6) membranes. As one sixth of the slope of the linear fitting for each MSD curve is diffusion coefficient, we calculate and list the results in the table. We can get from Fig. 4 (a) that the diffusion coefficient of water molecules in graphyne-N membrane systems gradually decreases with the increase of N (N=3, 4, 5, 6). In these systems, as the temperature and external pressure as well as the initial osmotic pressure difference are the same, the diffusion of water molecules are influenced by the hydrogen bonding interactions and the electrostatic forces as well as the Van der Waals forces caused by the surrounding water molecules, membranes and salt ions. Fig. 4 (a) and (b) show that the charge properties of graphyne-3 membrane and graphyne-4 membrane can promote the diffusion of water molecules in their FO systems, while the promoting effects of the charge properties of graphyne-5 membrane and graphyne-6 membrane on the diffusion of water molecules are not obvious due to their lower charge densities.

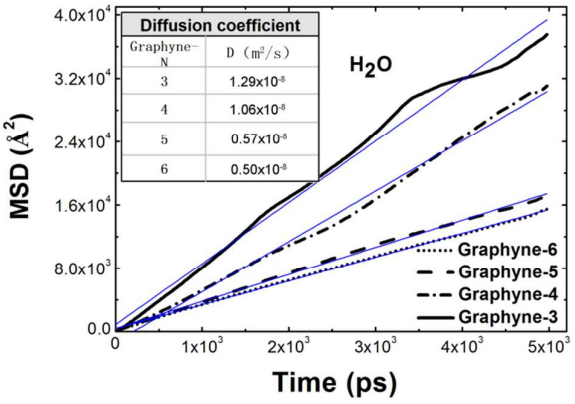

(a) Graphyne-N (N=3, 4, 5, 6)

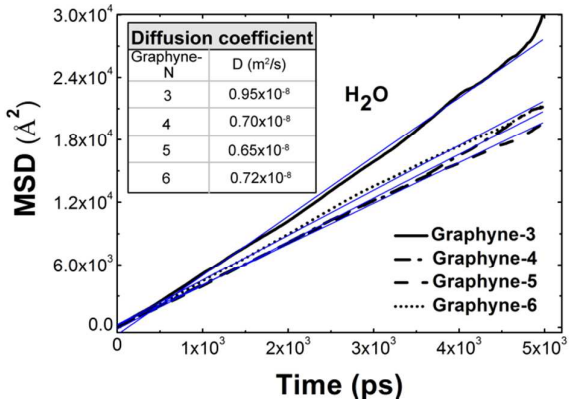

(b) Uncharged graphyne-N (N=3, 4, 5, 6)

Fig. 4 The mean square distance (MSD) curves of water molecules and corresponding fitting lines by least squares method *vs* simulation time and calculated values of diffusion coefficient in each system: (a) graphyne-N (N=3, 4, 5, 6); (b) uncharged graphyne-N (N=3, 4, 5, 6).

Fig. 5 (1) shows the distribution density of water molecules on the two sides of graphyne-N membrane in each system. We can see that water molecules are densely packed in the vicinity of the graphyne-N (N=3, 4, 5, 6) membranes, the distance from each membrane to the densely packed region is about 3.5 to 5.3 Å and the density gradually increase with N increase. Water is a structured liquid and hydrogen bonding network is formed in water bulk. The recent computer calculations have shown that the numbers of hydrogen bonds per water molecule at 298K-300K in water bulk are between 3.2 and 3.4 from molecular dynamic computations employing SPC/E water. [62] The four radial distribution function (RDF) curves in Fig. 5 (2) respectively show the density of hydrogen atoms surrounding every oxygen atom in these four systems. The calculation results show that the number of hydrogen bonds per water molecule in these four systems increases slowly with the increase of N, the values are

respectively 2.00, 2.09, 2.10 and 2.10 from N = 3 to N = 6. We can get that the water structures in these four systems have been disturbed compared with the pure water bulk, the numbers of hydrogen bonds per water molecule have decreased by about 1.1 to 1.4.

From Fig. 5 (1) and (2), we can get that the water structure in each graphyne-N (N = 3, 4, 5, 6) membrane system has been disturbed for the number of hydrogen bonds per water molecule is smaller than that of the pure water bulk. Several researchers have demonstrated that water molecules transport in a single file when they permeate through the pores of the graphyne membranes, the formation of two hydrogen bonds in the system is beneficial to the realization of that transmission mode. [37, 47, 48] The numbers of hydrogen bonds per water molecule are gradually away from the value of two from graphyne-3 membrane system to graphyne-6 membrane system, which leads to quantized transmission of water molecules become more difficult and the slowing down of the water transport with the increase of N. With the increase of N, although the pore diameter and porosity of graphyne-N membranes gradually increase, the quantized transmission of water molecules becomes more difficult. Besides, the charge properties of graphyne-N (N = 3, 4, 5, 6) membranes have different effects on the diffusion of water molecules. These comprehensive effects result in the trend of the water flux curve shown in Fig. 2.

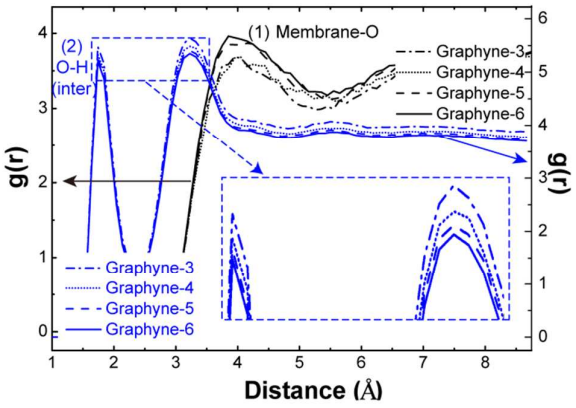

Fig. 5 (1) The radial distribution function (RDF) curves of water molecules on both sides of the membrane in these four systems. The position where the value of the distance equates 0 is the position where graphyne-N (N = 3, 4, 5, 6) membranes locate, and the figure below is the amplification of the marked peaks. (2) The RDF curves that reflect the distribution of water molecules relative to other water molecules in these systems, the two peaks respectively show the density of hydrogen atoms surrounding each water molecule which acts as benchmark.

3.3 Salt rejection by single-layer graphyne membranes in FO process

The Van der Waals diameters of sodium cations (Na^+) and chloride anions (Cl^-) are respectively 3.7 and 5.0 Å, the diameter of water molecule is 4.0 Å, and the effective Van der Waals diameters of the pores in graphyne-N (N=3, 4, 5, 6) membranes are respectively about 3.8, 5.4, 7.0 and 8.6 Å. [48] Considering the structure characteristics of water molecule and the diameter of each matter, we can get that water molecule and Na^+ are able to permeate through these four membranes, and Cl^- can permeate through graphyne-4, graphyne-5 and graphyne-6 membranes. However, Fig. 2 shows that graphyne-3 can simultaneously achieve perfect rejection for Na^+ and Cl^- , and graphyne-4, graphyne-5 as well as graphyne-6 can achieve a certain degree

of rejection for Na^+ and Cl^-. We can speculate from the above phenomenon that there may be some other factors hindering Na^+ and Cl^- from permeating through the membrane pores.

Fig. 6 shows the RDF curves that reflect the distribution of water molecules around Na^+ and Cl^-, the element (hydrogen atom or oxygen atom) corresponding to each peak and the values of r (the distance from ion center to the center of hydrogen atom or oxygen atom) have been pointed out. The two blue dotted lines respectively point out the locations of concentrated oxygen atoms within these two hydration shells around chloride anions. It shows that both Na^+ and Cl^- are surrounded by two hydration shells and the densities of the water molecules are different. We have worked out the coordination numbers of Na^+ and Cl^- by using the formula

$$N_{ij}(r) = 4\pi\rho_j \int_0^r r^2 \, g_{ij}(r) dr \quad (3.2)$$

Where $N_{ij}(\mathrm{r})$ is coordination number, ρ_j is the density of j in system, r is the distance between i and j, $g_{ij}(r)$ is the RDF of j with respect to i. The coordinate number in the first hydration shell of Na^+ and Cl^- are respectively about 5.2 and 6.2, the corresponding snapshots are shown in Fig. 6. This figure also shows that the diameters of the hydrated sodium cations and hydrated chloride anions are larger than the diameters of the graphyne-N (N=3, 4, 5, 6) membrane pores, indicating that only some water molecules in the hydration shells are stripped off can the hydrated ions permeate through the membrane pores. The formation of these hydrated ions leads to the separation of the salt and water. With the increase of N from 3 to 6, the pore diameter and porosity gradually increase, the numbers of water molecules

that should be stripped off in hydrated ions gradually reduce and the barriers triggered by size exclusion effect also gradually decrease, so both the rejection rate of Na^+ and Cl^- gradually decrease with the increase of N.

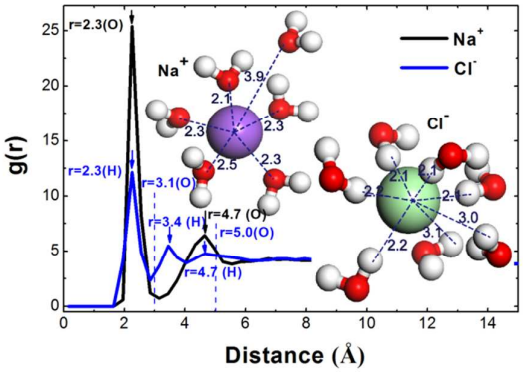

Fig. 6 The RDF curves of water molecules outside sodium ions and chloride ions. There are two hydration shells outside the sodium ion and the chloride ion. By calculating, the coordinate number in the first hydration shell of the hydrated sodium ions and hydrated chloride ions are respectively 5.2 and 6.2.

Furthermore, we can get from Fig. 7 that the rejection rate of both Na^+ and Cl^- of uncharged graphyne-N membrane are higher than or equal to that of the graphyne-N membrane when N = 3, 4, and 5, while the rejection rate of both Na^+ and Cl^- of uncharged graphyne-N membrane are lower than that of the graphyne-N membrane when N = 6. when N = 3, 4, and 5, the rejection rate of Na^+ is equal to that of the Cl^- for uncharged graphyne-N membrane, while the rejection rate of Na^+ is lower than that of the Cl^- for graphyne-N membrane. So we can get that the charge properties of graphyne-N membranes also have certain effects on the rejection rate of salts ions besides the size exclusion effect. These effects are relevant to electrostatic interactions between the carbon atoms of graphyne membranes and the salt ions or water

molecules.

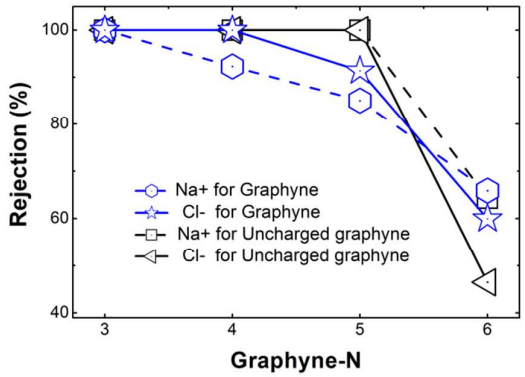

Fig. 7 Rejection rates of graphyne membrane and uncharged graphyne membrane *vs* membrane type, namely graphyne-N (N=3, 4, 5, 6).

3.4 Prospect for using graphyne membranes in water treatment

Experimental results show that the magnitude of the water flux of laboratory and commercial permeable membranes in RO or FO process are generally 10^{-3} when the units are L/(cm^2·h). [16, 20, 21] Simulation results in this paper show the magnitude of the water flux of single-layer graphyne membranes in FO process are 10 when the same units are used. The simulation conditions are comparable to those in experiments. It suggests that the difference in their water flux is about 4 orders of magnitude. As for laboratory and commercial permeable membranes, the total thickness of the dense selective layer and the support layer are tens to hundreds of microns and the thickness of the dense selective layer are tens to hundreds of nanometers.

When these polymeric membranes are used as selectively semipermeable membranes in FO processes, the concentration polarization phenomenon (both external concentration polarization (ECP) and internal concentration polarization (ICP)) will occur and the osmotic pressure difference across the membrane will be

much lower than the bulk osmotic pressure difference, which will lead to a great reduction of the water flux. In contrast, the Van der Waals thickness of the single-layer graphyne membranes are only one carbon atom in diameter, namely 3.4 Å. [63] When single-layer graphyne membranes are used in FO, the ICP which can markedly reduce water flux can be neglected, [37] the adverse effect of the ECP which plays a minor role in osmotic-driven membrane processes can be minimized by increasing flow velocity and turbulence at the membrane surface. [64] As graphyne membranes possess excellent chemical stability, membrane life will be greatly improved, which will save the expenditure for replacing osmosis membranes. For desalination, even considering the optimization of the draw solution and the benefits of reduced fouling during regeneration in FO, the energy efficiency of RO is likely to be superior to FO on account of the draw-dilution step in FO. But in regeneration-free applications or high salinity applications where the osmotic pressures of feeds are too great for existing reverse osmosis technologies, using graphyne membranes in FO is greatly superior to the use in RO [65].

Conclusion

We have studied the brine separation performance of graphyne-N (N = 3, 4, 5, 6) membranes in FO process by molecular dynamic simulation. Results show that single-layer graphyne-3 membrane can simultaneously achieve a high water flux and a rejection rate of 100%, which are also accompanied by a very high utilization of osmosis energy. There are no linear correlation between the water flux and the structure parameters including pore diameter and membrane porosity for graphyne-N

membrane systems in FO. The water structures in graphyne-N membrane systems have been disturbed for the numbers of hydrogen bonds per water molecule are smaller than that of the pure water bulk. The formation of the hydrated salt ions leads to brine separation to be achieved. The charge properties of graphyne-N membranes have certain effects on water transport and salt rejection. Owing to their naturally formed pores, high mechanical properties and excellent chemical and thermal stability, single-layer graphyne-N membranes have good prospects in brine separation, wastewater treatment, conservation and reuse of osmosis energy or regeneration-free applications for FO.

Acknowledgements

This work was supported by the National Natural Science Foundation of China (51473097), (51003067), the Opening Project of State Key Laboratory of Polymer Materials Engineering (Sichuan University) (sklpme2014-3-14), and the Fundamental Research Funds for the Central Universities (2012SCU04A03).

References

(1) J. Eliasson, Nature, 2015, 517, 6.

(2) M. Alamaro, Nature, 2014, 514, 7.

(3) C. Packer, R. Hilborn, A. Mosser, et al., Science, 2005, 307.

(4) C.J. Vörösmarty, P. Green, J. Salisbury, et al., Science, 2000, 289, 284-288.

(5) S. Kar, R.C. Bindal, P.K. Tewari, Nano Today, 2012, 7, 385-389.

(6) M. Elimelech, J. Water Supply: Research and Technology—AQUA | 55.1|.

(7) M. Park, J.J. Lee, S. Lee, et al., J. Membr. Sci. 2011, 375, 241-248.

(8) J.R. McCutcheon, R.L. McGinnis, M. Elimelech, J. Membr. Sci, 2006, 278, 114-123.

(9) J.R. McCutcheon, M. Elimelech, J. Membr. Sci, 2006, 284, 237-247.

(10) S. Zhang, K.Y. Wang, T.S. Chunga, et al., J. Membr. Sci, 2010, 360, 522-535.

(11) J.R. McCutcheon, R.L. McGinnis, M. Elimelech, Desalination, 2005, 174, 1-11.

(12) T.Y. Cath, A.E. Childress, M. Elimelech, J. Membr. Sci, 2006, 281, 70-87.

(13) L. Shi, S.R. Chou, R. Wang, et al., J. Membr Sci, 2011, 382, 116-123.

(14) J.R. McCutcheon, M. Elimelech, J. Membr. Sci, 2008, 318, 458-466.

(15) G. Han, T.S. Chung, M. Toriida, et al., J. Membr. Sci, 2012, 423-424, 543-555.

(16) L. Huang, N.N Bui, M.T. Meyering, et al., J. Membr. Sci, 2013, 437, 141-149.

(17) K.Y. Wang, T.S. Chung, R. Rajagopalan, Ind. Eng. Chem. Res, 2007, 46, 1572-1577.

(18) K.Y. Wanga, T.S. Chung, J.J. Qin, J. Membr. Sci, 2007, 300, 6-12.

(19) Q. Yang, K.Y. Wang, T.S. Chung, Environ. Sci. Technol. 2009, 43, 2800-2805.

(20) C.Q. Qiu, L. Setiawan, R. Wang, et al., Desalination, 2012, 287, 266-270.

(21) K.Y. Wang, R.C. Ong, T.S. Chung, Ind. Eng. Chem. Res, 2010, 49, 4824-4831.

(22) J.R. McCutcheon, M. Elimelech, J .AIChE, 2007, 53, 1736-1744.

(23) G.T. Gray, J.R. McCutcheon, M. Elimelech, Desalination, 2006, 197, 1-8.

(24) S. Joseph, N. R. Aluru, Nano Lett, 2008, 8, 2.

(25) Y.X. Jia, H.L Li, M. Wang, et al., Separation and Purification Technology, 2010, 75, 55-60.

(26) B. Corry, J. Phys. Chem. B, 2008, 112, 1427-1434.

(27) S. Kar, R.C. Bindal, P.K. Tewari, Nano Today, 2012, 7, 385-389.

(28) R.Das, M.E. Ali, S.B.A. Hamid, et al., Desalination, 2014, 336, 97-109.

(29) M.S. Mauter, M. Elimelech, Environ. Sci. Technol, 2008, 42, 16.

(30) M.E. Suk, N.R. Aluru, J. Phys. Chem. Lett, 2010, 1, 1590–1594.

(31) K. Sint, B. Wang, P. Kral, J. AM. CHEM. SOC, 2008, 130, 16448-16449.

(32) P.Z Sun, M. Zhu, K.L. Wang, et al., ACS Nano, 2013, 7, 1, 428-437.

(33) K. Celebi, J. Buchheim, R.M. Wyss, et al., Science, 2014, 344, 18.

(34) S.C.O. Hern, M.S.H. Boutilier, J.C. Idrobo, et al., Nano Lett, 2014, 14, 1234-1241.

(35) C.T. David, J.C. Grossman, Nano Lett, 2012, 12, 3602-3608.

(36) J.G. Gai, X.L. Gong, W.W. Wang, et al., J. Mater. Chem. A, 2014, 2, 4023-4028 | 4023.

(37) J.G. Gai, X.L. Gong, J. Mater. Chem. A, 2014, 2, 425-429 | 425.

(38) S. Bae, H. Kim, Y. Lee, et al., Nat. Nanotechnol., 2010, 5, 574.

(39) X. Li, W. Cai, J. An, et al., Science, 2009, 324, 1312.

(40) T. Hesjedal, Appl. Phys. Lett., 2011, 98, 13, 3106.

(41) T. Yamada, M. Ishihara, J. Kim, et al., Carbon, 2012, 50, 3, 2615.

(42) T. Kobayashi, M. Bando, N. Kimura, et al., Applied Physics Letters, 2013, 102: 023112.

(43) S.P. Surwade, S.N. Smirnov, I.V. Vlassiouk, et al., Nature nanotechnology, DOI: 10.1038/NNANO.2015.37.

(44) M.S.H. Boutilier, C.Z. Sun, S.C. O'Hern, et al., ACS Nano, 2014, 8, 841.

(45) F. Perreault, A.F. de Faria, M. Elimelech, Chem. Soc. Rev., 2015, DOI: 10.1039/c5cs00021a.

(46) J.L. Kou, X.Y. Zhou, Y.Y. Chen, et al., J. Chem. Phys, 2013, 139, 064705.

(47) C.Q. Zhu, H. Li, X.C Zeng, et al., Scientific Reports, 2013, 11, 1-7.

(48) S.C. Lin, M.J. Buehler, Nanoscale, 2013, 5, 11801.

(49) J.L. Kou, X.Y. Zhou, H.J. Lu, et al., Nanoscale, 2014, 6, 1865.

(50) M.M. Xue, H. Qiu, W. L. Guo, Nanotechnology, 2013, 50, 5720.

(51) Y.L. Yang, X.M. Xu, Computational Materials Science, 2012, 61, 83-88.

(52) S.W. Cranford, D.B. Brommer, M.J. Buehler, Nanoscale, 2012, 4, 7797.

(53) Q. Yue, S.L. Chang, J. Kang, et al., J. Phys. Chem. C, 2013, 117, 14804-14811.

(54) S.W. Cranford, M.J. Buehler, Carbon, 2011, 49, 4111-4121.

(55) A .L. Ivanovskii, Progress in Solid State Chemistry, 2013, 41, 1-19.

(56) Y.J. Li, L. Xu, H.B. Liu, et al., Chem. Soc. Rev, 2014, 43, 2572-2586.

(57) Y. Tobe, K. Kubota, K. Naemura, J. Org. Chem., 1997, 62, 3430-3431.

(58) H. Nishide, M. Takahashi, J. Takashima, et al., J. Org. Chem., 1999, 64, 7375-7380.

(59) Y. Tobe, I. Ohki, M. Sonoda, et al., J. Am. Chem. Soc., 2003, 125, 5614-5615.

(60) Li G, Li Y, Liu H, et al., Chem. Commun., 2010, 46, 3256.

(61) M.G. Hill, Membrane Technology And Applications, ed. R.W. Baker, 2nd edn, 2004, 1-534.

(62) M. Yizhak, Chem. Rev. 2009, 109, 1346-1370.

(63) J.M. Ducéré, C. Lepetit, R. Chauvin, J. Phys. Chem. C, 2013, 117, 21671-21681.

(64) T.Y. Cath, A.E. Childress, M. Elimelech, J. Membr. Sci, 2006, 281: 70–87.

(65) R. K. McGovernn and J. H. Lienhard V, J. Membr. Sci, 2014, 469: 245 – 250.